CHALMERS

Chalmers Publication Library

Graphene oxide and adsorption of chloroform: A density functional study

This document has been downloaded from Chalmers Publication Library (CPL). It is the author´s version of a work that was accepted for publication in:

Journal of Chemical Physics (ISSN: 0021-9606)

Citation for the published paper:
Kuisma, E. ; Hansson, F. ; Lindberg, B. et al. (2016) "Graphene oxide and adsorption of chloroform: A density functional study". Journal of Chemical Physics, vol. 144(18), pp. Art. no. 184704.

http://dx.doi.org/10.1063/1.4948321

Downloaded from: http://publications.lib.chalmers.se/publication/238980

Notice: Changes introduced as a result of publishing processes such as copy-editing and formatting may not be reflected in this document. For a definitive version of this work, please refer to the published source. Please note that access to the published version might require a subscription.

Chalmers Publication Library (CPL) offers the possibility of retrieving research publications produced at Chalmers University of Technology. It covers all types of publications: articles, dissertations, licentiate theses, masters theses, conference papers, reports etc. Since 2006 it is the official tool for Chalmers official publication statistics. To ensure that Chalmers research results are disseminated as widely as possible, an Open Access Policy has been adopted.
The CPL service is administrated and maintained by Chalmers Library.

(article starts on next page)

Graphene oxide and adsorption of chloroform: a density functional study

Elena Kuisma, C. Fredrik Hansson, Th. Benjamin Lindberg, Christoffer A. Gillberg, Sebastian Idh, and Elsebeth Schröder[a)]

Quantum Device Physics Laboratory, Microtechnology and Nanoscience (MC2), Chalmers University of Technology, SE-412 96 Göteborg, Sweden

(Dated: April 5, 2016)

Chlorinated hydrocarbon compounds are of environmental concerns, since they are toxic to humans and other mammals, are widespread, and exposure is hard to avoid. Understanding and improving methods to reduce the amount of the substances is important. We present an atomic-scale calculational study of the adsorption of chlorine-based substance chloroform ($CHCl_3$) on graphene oxide, as a step in estimating the capacity of graphene oxide for filtering out such substances, e.g., from drinking water. The calculations are based on density functional theory (DFT), and the recently developed consistent-exchange functional for the van der Waals density-functional method (vdW-DF-cx) is employed. We obtain values of the chloroform adsorption energy varying from roughly 0.2 to 0.4 eV per molecule. This is comparable to previously found results for chloroform adsorbed directly on clean graphene, using similar calculations. In a wet environment, like filters for drinking water, the graphene will not stay clean and will likely oxidize, and thus adsorption onto graphene oxide, rather than clean graphene, is a more relevant process to study.

Keywords: graphene oxide, chloroform, vdW-DF, vdW-DF-cx, van der Waals, DFT, adsorption, water filtering, water cleaning

I. INTRODUCTION

Graphite oxide was first synthesized more than 150 years ago[1] but caught general interest[2–16] only during the past few decades when research in 2D materials, in particular graphene, has started to bloom. Graphite oxide is an alternative path to large-scale production of graphene, by liquid-phase exfoliation of graphite oxide into layers, called graphene oxide (GO), and subsequent reduction to graphene,[2–4] but already the GO sheets have intriguing and useful features. GO can be understood as functionalized graphene, oxidized with hydroxyl, epoxide and some carboxyl groups. Its properties depend on the details of the oxidation: the type of, the number of and the distribution of the functional groups. GO has tuneable electric properties, obtained by changing the functional groups, and with its thin size could be used for electronics.[5] GO is highly catalytic, highly solvable in water and other solvents, and is proposed for use as a gas sensor.[14]

GO has been suggested as a material for use in filtering of toxic compounds,[15,16] such as chlorinated hydrocarbon compounds. These are some of today's environmental concerns, since they are toxic to both humans and other mammals, and exposure is hard to avoid. Exposure to chlorine-based compounds arises, e.g., from consumption of chlorinated drinking water or food supplies that have been contaminated by residues of industrial chemicals.[17,18]

We present a computational study of GO with state-of-the-art calculations, using a recent implementation of density functional theory (DFT). We study how GO binds chloroform, one of the common chlorine-based substances, by calculating the binding energy and its dependence on the structure of GO.

GO has previously been studied[6–11] in experiments and by use of calculational tools, including DFT. The GO itself is expected to be reasonably well described[12] by use of semilocal approximations of the exchange and correlation of DFT, such as in the PBE approximation,[19] but for our subsequent studies of chloroform physisorption it is imperative that the dispersive nonlocal interactions be included in a consistent way. Therefore we here use the van der Waals (vdW) density functional method[20–24] (vdW-DF), in the vdW-DF-cx version,[23,25] for all calculations except for a comparison with previous results, where we use PBE for some calculations.

Chloroform with graphitic or other carbon based materials was previously studied in a couple of experimental and computational studies.[26–30] Also, a DFT based study of ammonia adsorption was presented earlier.[31] However, to our knowledge there are no previously DFT studies of chloroform adsorption on GO using methods that include the vdW interactions consistently, such as here. Certainly, physisorption of chloroform on GO with the recent vdW-DF-cx has not previously been covered.

This article is structured as follows: In Section II we describe the method of computation and the systems studied. In Section III the results are presented and discussed, along with a discussion of the accuracy of our calculations, and Section IV summarizes the study.

II. PHYSICAL SYSTEM AND COMPUTATIONAL METHOD

In the following we describe GO and its functional groups and how we model the relevant parts of GO in our adsorption study. We also describe the methods used for

---

[a)] Electronic mail: schroder@chalmers.se the DFT calculations and define the binding energies for the functional groups in GO and for chloroform on GO, including a discussion of what constitutes the zero point of the binding energies in these calculations. This varies in the literature, making comparison difficult.

A. GO and chloroform

GO has a graphene carbon network with an almost amorphous distribution of functional groups, and it is difficult to determine the types of functional groups present and their positions. In Ref. 6 Lerf et al. used reactions with various reagents to supplement their previous NMR measurements. They found that graphite oxide (and thus likely also GO) mainly has two types of functional groups: O bound in the C-C bridge site, which is the 1,2-ether or epoxide, and the C-OH or hydroxyl group. They also found no support for O bound to two next-nearest neighbor C atoms (the 1,3-ether) and very little for the carboxyl (the -COOH) group. Based on their measurements they put forward a structural model for GO that has areas without functional groups (i.e., areas of clean graphene) and other areas with epoxide and hydroxyl groups randomly distributed but close together. In their model the carbon grid of GO is almost flat, except for the parts where C atoms are attached to hydroxyl. The GO has functional groups on both sides of the carbon grid and carboxyl groups are only present at the edges of GO.

In experiments, fully oxidized GO is found to have a C:O ratio approximately 2:1 or more.[32] However, GO is not always found in the fully oxidized state. Even though the GO model of Lerf et al.[6] has a relatively high concentration of functional groups, the C:O ratio is only about 5:1 in the areas that are not part of the GO sheet edges.

In the present study of GO we consider structures with clusters of functional groups on otherwise clean graphene, the clusters being relatively small and disordered. Thus, we compute the structures and energies involved in the formation of epoxide and hydroxyl groups on graphene for GO with low O concentration (C:O ratio from 72:1 to 15:1). Guided by the findings by Lerf et al. we use GO with functional groups on either both sides of the carbon grid (not symmetrically positioned) or one side with just a few clustered groups only. In our study we use periodic boundary conditions in space and thus the GO has no edges. This means that according to the model by Lerf et al. there should not be any carboxyl groups included.

Chloroform ($CHCl_3$) consists of a central carbon atom with three electronegative Cl atoms in a ‘tripod’ in one end and a H atom at the other end. This gives chloroform a finite dipole moment, which affects its physisorption properties.

In our chloroform adsorption study we initially studied mainly (but not exclusively) GO structures that have all functional groups on the same side as the adsorbed molecule because these groups were supposedly the ones that influence the chloroform-GO binding the most. However, we see that also groups on the other side of the carbon grid affect the adsorption energy and our study has been enlarged to enclose also systems with functional groups on both sides.

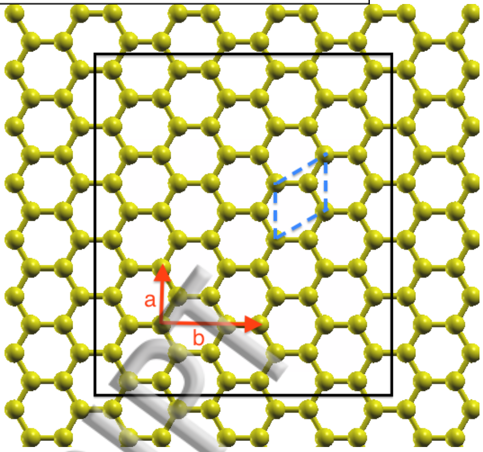

FIG. 1. Graphene slab. The unit cell (area delimited by the black solid line) used in this study consists of 3 × 6 conventional rectangular graphene cells, each containing four carbon atoms, double the size of the primitive unit cell (blue dashed line). The lengths of unit vectors (red solid arrows) of the conventional cell are $a = 2.456$ Å and $b = a\sqrt{3} = 4.254$ Å. Visualization (here and in Figures 3, 4 and 6) using XCrySDen.[33]

B. Unit cell

To study GO we start out with a graphene slab with added functional epoxide and hydroxyl groups. We use a $3\sqrt{3} \times 6$ orthorhombic unit cell with 72 graphene C atoms, as illustrated in Figure 1, with a C-C distance of 1.424 Å, and periodic boundary conditions. The unit cell height is varied such that the amount of vacuum between each copy of the system is approximately 10 Å, thus for clean GO calculations the unit cell height is 10.5 Å, and approximately 15.5 Å for physisorption of chloroform on GO. In the calculations of adsorbed chloroform the molecule-molecule nearest-neighbor distance is 12.8 Å (the unit cell width) and the smallest lateral distance between any two atoms in neighboring chloroform molecules is 10.4 Å, as illustrated in Figure 2.

C. Methods of computation

The formation of GO from graphene is a process in which hydroxyl and epoxide groups chemisorb on graphene. Such processes are expected to be well described with a semilocal density functional like PBE.[19] However, the adsorption of chloroform on GO is a physisorption process and in such processes a robust de-

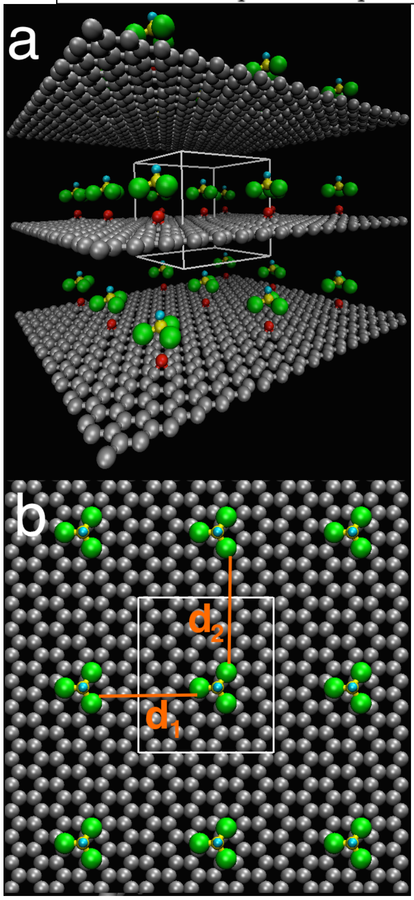

FIG. 2. Sketch of the unit cell used for calculations of chloroform adsorption on GO. The size of the unit cell (white box) is approximately $12.8 \times 14.8 \times 15.5$ Å. *Color legend:* Chloroform has yellow C; lime Cl; blue H, and GO has gray C; red O. Closest atom-atom distances between chloroform molecules are indicated, $d_1 = 10.4$ Å and $d_2 = 11.9$ Å. Visualization using VMD.[34]

scription of the dispersive interactions is necessary. We therefore perform the main DFT calculations using the vdW-DF method[20–24] in the consistent exchange vdW-DF-cx version.[23,25] The vdW-DF-cx functional has been shown to work well for layered structures and aromatic molecules, and it accurately predicts the a and c lattice constants of solid graphite.[23] It thus provides a balanced description between the chemical sp^2 bonding within the graphene sheets and the vdW interactions between layers and in physisorption.

To describe the GO used as a substrate it is important that the method we use can also handle the balance between sp^2 and sp^3 binding, in the graphene patches and at the sites of the functional groups, respectively. The fact that vdW-DF-cx shows reasonable results for the phase transition between diamond and graphite, which are sp^3 and sp^2 materials, is encouraging.[23] To further document the ability of vdW-DF-cx for this problem we compare formation energies for a number of unsaturated GO configurations, obtained with both the vdW-DF-cx and the semilocal PBE functional.

For the calculations of vdW-DF-cx and PBE results we use QUANTUM ESPRESSO[35,36] (QE), and all calculations are carried out self-consistently. We use ultrasoft pseudopotentials[37,38] with wavefunction and density cutoff energies 30 and 120 Ry, respectively, except when calculating the effect of spin on the total energies of O and OH where we instead use the values 80 and 320 Ry. The force convergence threshold value is set to 2 meVÅ^{-1}, and the number of **k**-points is $4 \times 4 \times 1$ (and $1 \times 1 \times 1$ for small molecules). These values are chosen after a careful check of the binding energy convergence, as further described towards the end of Section III B.

The binding energy of the epoxide and hydroxyl functional groups on graphene is calculated with respect to the sum of energies of clean graphene and isolated O and OH in vacuum

$$E_b = -(E_{\mathrm{GO}} - E_{\mathrm{G}} - nE_{\mathrm{O}} - mE_{\mathrm{OH}})\,. \qquad (1)$$

Here E_{GO} and E_{G} are the total energies of GO and graphene, and E_{O} and E_{OH} are the total energies of isolated O and OH, with n and m the number of epoxides and hydroxyl groups in the GO. E_b is defined positive for systems that bind.

For the graphene and GO constituents of (1) we use spin-balanced calculations, i.e., we ignore the effect of spin, which is small. On the other hand, for the isolated O and OH parts we do need to allow for spin-polarization in the calculations. Since spin calculations require more stringent convergence criteria we lift out the spin calculations to only deal with the isolated O atoms or isolated OH groups:

$$\begin{aligned} E_b &= -\left(E^{\mathrm{s}}_{\mathrm{GO}} - E^{\mathrm{s}}_{\mathrm{G}} - nE^{\mathrm{s}}_{\mathrm{O}} - mE^{\mathrm{s}}_{\mathrm{OH}}\right) & (2)\\ &\approx -\Big(E^{\mathrm{ns}}_{\mathrm{GO}} - E^{\mathrm{ns}}_{\mathrm{G}} - nE^{\mathrm{ns}}_{\mathrm{O}} - n\left(E^{\mathrm{s}}_{\mathrm{O}} - E^{\mathrm{ns}}_{\mathrm{O}}\right)^{\mathrm{high}} \\ &\quad -mE^{\mathrm{ns}}_{\mathrm{OH}} - m\left(E^{\mathrm{s}}_{\mathrm{OH}} - E^{\mathrm{ns}}_{\mathrm{OH}}\right)^{\mathrm{high}}\Big)\,, & (3) \end{aligned}$$

where superscripts s and ns denote "allowing for spin-polarization" and "spin-balanced". Superscript "high" denotes high (stringent) accuracy, which here means that the wavefunction and electron density energy cutoffs are 8/3 times higher than those of the ordinary spin-balanced calculations.

The chloroform-on-GO calculations are carried out without considering spin, with spin-balanced calculations of chloroform and of graphene making up the two individual parts of the reference energy.

In the results section we report the height h of the chloroform molecule above GO in the adsorbed position. The height is taken as the projection in the z-direction (i.e., perpendicular to graphene) of the distance between the chloroform C atom and the nearest GO surface O atom. This means that an atom in chloroform may be closer to the GO O-atom than the distance h.

III. RESULTS AND DISCUSSION

A. Oxidized graphene

We focus on lightly oxidized graphene, with only a few functional groups per 72 C-atom unit cell. We use 10 different configurations with up to three epoxide groups and up to two hydroxyl groups per unit cell, as illustrated in the left hand side of Figure 3. The functional groups are placed such that they form clusters, as expected from experiments.[6] The resulting binding energies are presented in the graph on the right hand side and in Table I. Structures GO1–3 and GO6–9 have groups on one side of the graphene plane only, structures GO4–5 have one epoxide on each side, and structure GO10 has epoxide and hydroxyl groups on both sides. The C–O lengths for the epoxides and hydroxyl groups are 1.47 Å and 1.52 Å with the vdW-DF-cx functional.

By studying the binding energy E_b for each structure we find that E_b has an almost linear dependence on number of C atoms involved in binding the functional groups: the right hand side of Figure 3 shows that for every C atom involved (meaning there will be one less sp^2-bound C atom) E_b increases by almost 1.5 eV. For comparison, one single hydroxyl group has a binding energy of about 0.9 eV and the epoxide group, with its two C-O bonds, has a binding energy of about 2.2 eV, so the gain in adding a functional group to a cluster is significantly higher, per C-O bond, than just adding the group to a patch of clean graphene. There is some spread in the numbers, and the illustrations of the structures show that the clusters of functional groups are not all densely packed, leading to less gain in energy for sparse clusters than for more dense clusters.

The preference for having functional groups in clusters is seen already in a cluster of two hydroxyl groups: we see a huge gain in energy (almost 0.9 eV) by pairing hydroxyl groups, instead of having them separated. This is so even when the groups are on the same side of the graphene grid and give rise to more distortion of the graphene than the distortion created by one single hydroxyl group (structure GO6 compared to GO2 times 2).

More generally, by visually comparing all of the structures in the left hand side of Figure 3 we find that structures with groups on both sides (GO4, GO5, and GO10) have a less distorted carbon structure than structures with groups only on one side (all others), as expected.[9]

Table II shows that for structures with two epoxides (GO3, GO4, and GO5) an energy gain can be obtained both by clustering, with gain per O atom 0.31 eV (from comparing GO1 and GO4), and by having the epoxide groups on both sides of the graphene instead of one side (gain 0.11 eV). However, we also see that the largest gain is obtained by having the epoxides as nearest neighbors as opposed to next-nearest neighbors (gain 1.11 eV). This is seen to be independent of DFT method used (vdW-DF-cx and PBE) and can also be seen in literature values.[39]

TABLE I. Binding energy E_b and binding energy per O atom E_b/O of epoxide (O) and hydroxyl (OH) groups on graphene, calculated using the vdW-DF-cx and PBE functionals. Energies in units of eV. See Figure 3 for the systems GO#.

GO#	GO struct.	E_b^{cx}	E_b^{cx}/O	E_b^{PBE}	E_b^{PBE}/O
GO1	O	2.156	2.156	2.166	2.166
GO2	OH	0.918	0.918	0.769	0.769
GO3	2O	4.818	2.409	4.844	2.422
GO4	2O	4.931	2.466	4.937	2.469
GO5	2O	3.819	1.910	3.831	1.916
GO6	2OH	2.700	1.300	2.495	1.247
GO7	2O, OH	6.172	2.057	6.042	2.014
GO8	O, 2OH	4.494	1.498	4.189	1.396
GO9	3O, 2OH	9.872	1.984	9.592	1.918
GO10	3O, 2OH	10.751	2.150	10.412	2.083

Returning to the full set of formation energy results, Table I, we can compare the results of PBE calculations to vdW-DF-cx calculations. The PBE calculations are expected to get both the sp^2 and sp^3 binding of the C atoms reasonably correct (but not so for the long-range interactions, which are important in chloroform physisorption). We find that the vdW-DF-cx formation energies are systematically stronger than those of PBE, with up to 19% difference in formation energies. However, the difference depends on the type of functional group(s) involved in the GO structure: for epoxides the difference in formation energy of vdW-DF-cx compared to PBE is from practically identical (on the meV scale), to maximum 5%, whereas the difference is 4–19% for hydroxyl groups, and mixed structures in the range 2–7%.

It is important to note that these differences in vdW-DF-cx and PBE formation energies *include* differences caused by differing positions of the atoms when structurally relaxing the atomic positions in either vdW-DF-cx or PBE. The hydroxyl functional group has an H atom pointing away from graphene, this makes long-range interactions more relevant for hydroxyl than for the epoxide. The single-bonded H atom also has a less stiff binding, and small changes in the forces on the atoms (from change of functional) can more easily move the H atoms than the more stiffly bound O atoms. These differences between the hydroxyl and epoxide functional groups are likely at least part of the reason for the larger PBE to vdW-DF-cx energy difference when hydroxyl groups are involved: vdW-DF-cx may actually turn out to describe those groups better than PBE! However, without experiments or high-quality quantum chemistry calculations to compare to we cannot claim that this is the case.

We notice that the binding energy in (3) is calculated relative to the open-shell O atom and OH radical, computed in vdW-DF-cx or PBE. It is possible to convert the numbers obtained for E_b into energies given with respect to the closed shell molecules H_2O and H_2, Ref. 40. This

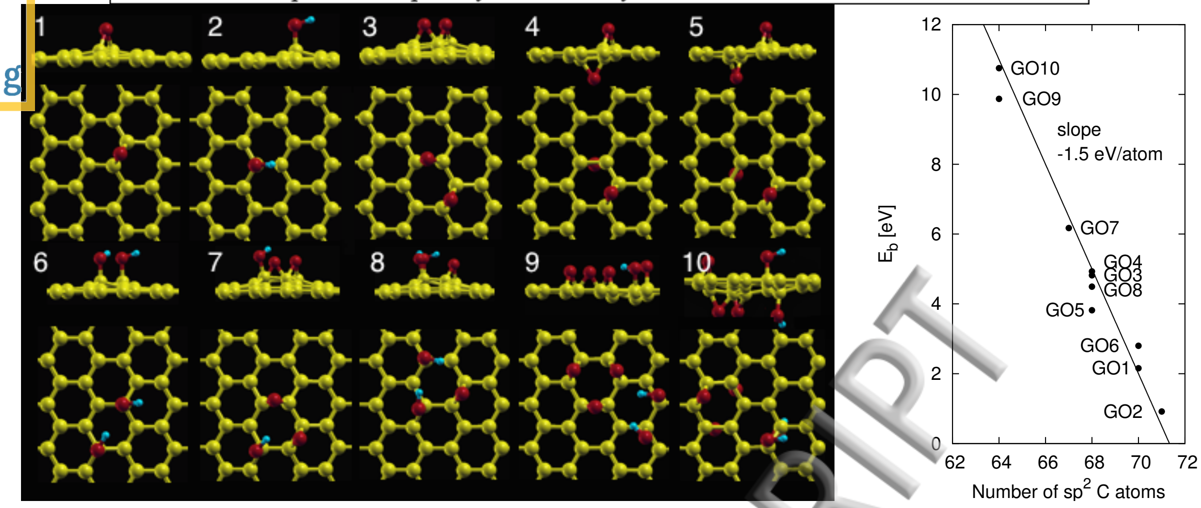

FIG. 3. Left: Epoxide and hydroxyl groups on graphene. The top and side views of optimized geometries of systems GO1–10. Only a part of the unit cell is shown. *Color legend for atoms:* yellow C; red O; blue H. Right: The corresponding binding energies, as also presented in Table I, as a function of C atoms in the unit cell not bound to functional groups, i.e., number of remaining sp^2 C atoms of the initial 72 C atoms in the clean graphene. The method vdW-DF-cx is used for the structures shown here.

TABLE II. Binding energies E_b and energy differences for GO structures with two epoxide groups, systems GO3, GO4 and GO5 and a single epoxide group, GO1. Calculations performed with the vdW-DF-cx and PBE functionals. The structures differ by having epoxide on one (GO3) or both sides (GO4) of the graphene plane, and by having the epoxides placed as nearest neighbors (GO4) or across the graphene carbon ring (GO5). The literature values (Ref. 39) are for similar but not identical systems. All energies in units of eV.

Structure	vdW-DF	PBE	PBE, Ref. 39
GO3	4.82	4.84	
GO4	4.93	4.94	4.76
GO5	3.82	3.83	3.59
GO4−GO3	0.11	0.10	
GO4−GO5	1.11	1.11	1.17
GO4−2×GO1	0.62	0.61	

conversion is obtained by adding to E_b the numbers

$$\Delta_{\mathrm{O}} = E^{\mathrm{ns}}_{\mathrm{H_2O}} - E^{\mathrm{ns}}_{\mathrm{O}} - (E^{\mathrm{s}}_{\mathrm{O}} - E^{\mathrm{ns}}_{\mathrm{O}})^{\mathrm{high}} - E^{\mathrm{ns}}_{\mathrm{H_2}}) \qquad (4)$$

$$\Delta_{\mathrm{OH}} = E^{\mathrm{ns}}_{\mathrm{H_2O}} - E^{\mathrm{ns}}_{\mathrm{OH}} - (E^{\mathrm{s}}_{\mathrm{OH}} - E^{\mathrm{ns}}_{\mathrm{OH}})^{\mathrm{high}} - \frac{1}{2}E^{\mathrm{ns}}_{\mathrm{H_2}} \qquad (5)$$

for every epoxide or hydroxyl group. For vdW-DF-cx (PBE) the two numbers are −5.363 eV and −3.010 eV (−5.670 eV and −3.145 eV).

B. Adsorption of chloroform

The main goal is to examine how chloroform binds to GO. Our focus is on studying the effect on the binding energy of the presence of and the positions of the epoxide and hydroxyl groups and the relative orientation of the chloroform molecule. Since GO is almost amorphous an exhaustive search is prohibitive. Instead only the few functional groups closest to the chloroform molecule are examined, keeping the rest of the unit cell clean of functional groups (i.e., using graphene), even if that might result in a slightly worse binding energy than on fully oxidized GO. For the orientation of chloroform we consider adsorption with the H atom pointing away from the GO (“H up”) or towards the GO (“H down”), being aware that in the end positional relaxation due to the Hellmann-Feynman forces on the atoms moves the groups and molecules to less well-defined orientations.

Several configurations of chloroform on GO are studied, and data for 16 of these systems are presented in Figure 4 and Table III. The GO structures are mainly those presented in Figure 3 and Table I, plus a few others.

Overall the chloroform adsorption energy lies approximately in the range 0.2–0.4 eV. A closer look on the various adsorption systems compared for similarities yields the following insights: System I compared to system II shows that adsorption close to an (isolated) epoxide is more favorable by about 0.08 eV than adsorption close to an (isolated) hydroxyl. The systems III, IV, and V compared to I show that adsorption close to a pair of epoxides is more favorable than adsorption on a single epoxide. The gain depends on the relative positions of the epoxides: if they are on the same side of the graphene plane (III and V) the chloroform adsorption energy is 0.11 eV less (i.e., adsorption less favorable) than if the epoxides are not on the same side (IV); if the epoxides are in nearest-neighbor positions (III) the chloroform adsorption energy is 0.04 eV less than if the epoxides sit

AIP Publishing

across the C 6-ring (V).

Systems VI and VII are used to examine the dependence on the relative positions of hydroxyl pairs: in these calculations positioning the hydroxyl pair across a C 6-ring is favorable for the chloroform adsorption by 0.19 eV. Adsorption on two hydroxyl is also clearly preferable to adsorption on one hydroxyl only (II), by 0.20 eV.

With more complex systems of functional groups in the model of GO it is less clear which properties of the GO affect the adsorption the most. We can, however, examine whether having the chloroform H atom pointing towards or away from GO is favorable. For clean graphene it has previously been found that an orientation with H pointing away from graphene and the Cl-Cl-Cl tripod pointing towards graphene is most favorable, among the orientations considered, such as the Cl-Cl-H tripod pointing towards graphene, or the H atom pointing towards graphene.[29] Because of the more uneven structure of the GO surface, compared to clean graphene with very little corrugation, we cannot distinguish between the orientation with the chloroform H atom pointing to GO and the Cl atoms all pointing away, and the orientation with the Cl-Cl-H tripod pointing to GO. We will therefore here only distinguish the situations of chloroform H pointing mainly away from GO (“H up”) from H pointing mainly towards GO (“H down”).

Systems VIII and IX differ in principle only by the orientation of chloroform (besides the thus induced positional relaxations of both the GO and the chloroform atoms). The adsorption energies of these systems indicate that “H down” is preferable. However, results for the more complex systems X, XI and XII clearly show that for those systems the “H up” orientation is more favorable, at least if there are functional groups on both sides of the graphene plane, but also that it matters how the Cl atoms are positioned relative to the atoms in the epoxide.

Systems XIV, XV and XVI all have the same number of functional groups, placed either on one or both sides of the graphene plane. Again, the data show that placing functional groups on both sides of the plane is preferable, even when the number of functional groups are restricted and the number of functional groups close to chloroform thus becomes less, compared to having all groups on the same side as the chloroform.

The measure h in Table III is an indication of the distance of chloroform from GO. Since GO is not flat, this measure is may be both shorter or longer than the smallest atom-to-atom distance for an atom in chloroform to an atom in GO. The h measures the distance between the chloroform C atom and the closest GO O-atom, projected onto the direction perpendicular to the underlying graphene. The values of h in our calculations fall in the range 2.1 to 3.8 Å. These are reasonable distances for physisorption.

The adsorption of chloroform on clean graphene, without functional groups, was previously obtained[29] as 0.36 eV using a similar method. This value corresponds well to the most favorable configurations for chloroform on GO systems studied here.

TABLE III. Binding energies E_b of chloroform on GO and height h of chloroform above a GO O-atom (see Figure 4 for the GO-chloroform system numbers). GO# refers to the GO structures of Figure 3 and Table I.

System	CCl_3H orient.	GO struct.	GO#	E_b [eV]	h [Å]
I	H up	O	GO1	0.257	3.34
II	H up	OH	GO2	0.181	3.45
III	H up	2O	GO3	0.225	3.56
IV	H up	2O	GO4	0.382	2.72
V	H up	2O	-	0.268	3.40
VI	H up	2OH	-	0.390	2.14
VII	H up	2OH	GO6	0.199	3.69
VIII	H up	2O, OH	GO7	0.219	3.81
IX	H down	2O, OH	GO7	0.286	3.12
X	H down	O, 2OH	-	0.319	2.99
XI	H down	O, 2OH	-	0.296	2.99
XII	H up	O, 2OH	-	0.422	2.44
XIII	H up	2O, 2OH	-	0.243	3.45
XIV	H up	3O, 2OH	GO9	0.275	3.79
XV	H up	3O, 2OH	GO10	0.333	2.88
XVI	H up	3O, 2OH	-	0.391	2.59

We carefully check the convergence of parameters used in our calculations. For one of the chloroform adsorption systems (System II in Figure 4) we change the parameter values, one by one, to slightly better and slightly worse values, and calculate the binding energy. In Figure 5 we report the binding-energy dependence on unit cell size, wavefunction and density cut-off energies, the force convergence threshold value, the number of **k**-points, and the vacuum size. The corresponding parameters are represented as a series of calculations, in which the accuracy increases going from left to right in the figure. The parameter values chosen from this convergence test for production runs are more accurate than the default values of QE. The convergence tests show that further improvements of the parameters, than what we have used in this study, result in changes of adsorption energies of a few meV or less, i.e., negligible improvements.

C. Effect of water

In the calculations presented here GO and chloroform are in vacuum. In a water-filter situation there will, obviously, also be water molecules present. How does water affect our chloroform adsorption results (Table III)?

One part of the total energy in vdW-DF-cx calculations is the nonlocal correlation energy,[20,24] E_c^{nl}. In the adsorption considered here, the change in E_c^{nl} before and after the adsorption $\{-\Delta E_c^{nl}$, with appropriate sign to fit the definition of E_b in (1)–(3)$\}$ dominates the binding

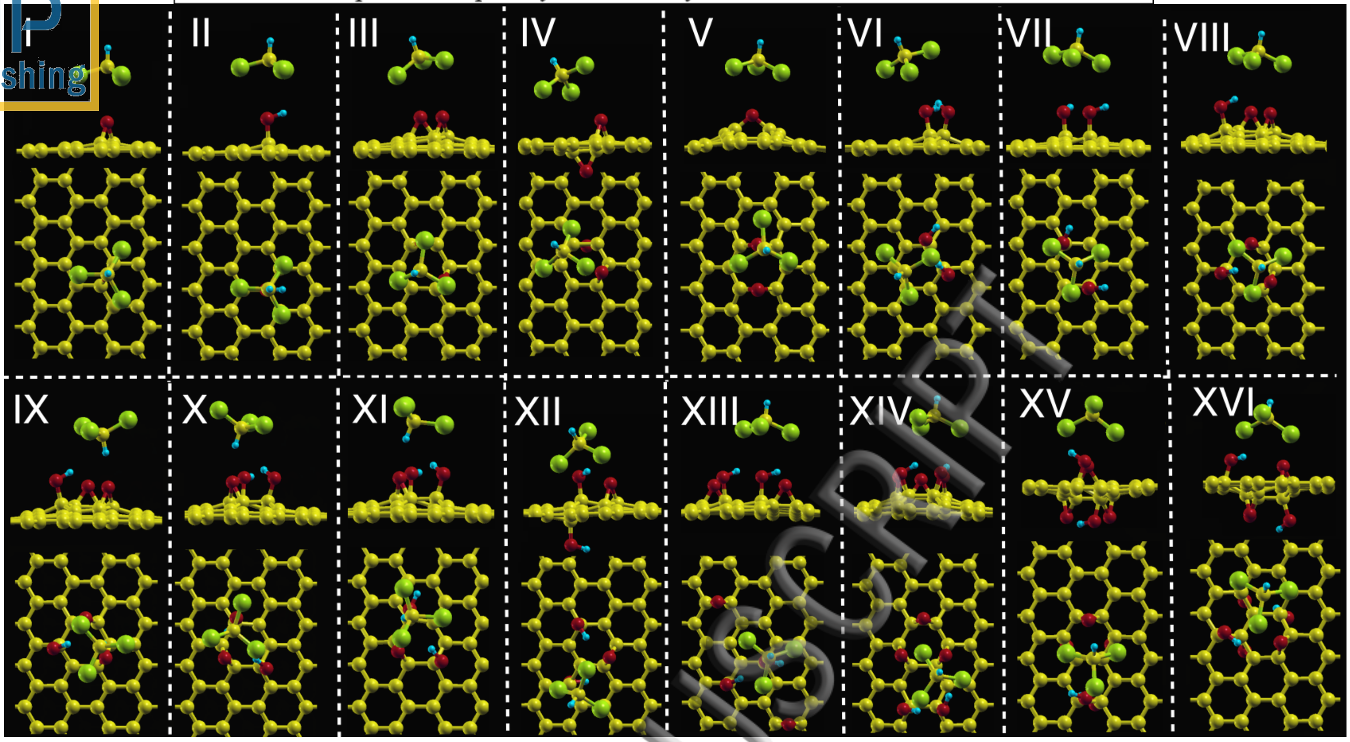

FIG. 4. Adsorption of chloroform on GO. Shown are top and side views of optimized geometries in systems I–XVI, obtained with the method vdW-DF-cx. Only a part of the unit cell is shown. The corresponding binding energies are presented in Table III. *Color legend for atoms:* green Cl; yellow C; red O; blue H.

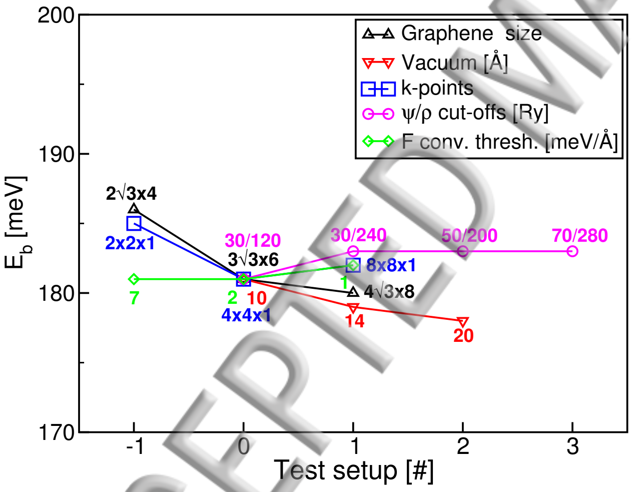

FIG. 5. Convergence tests of calculations for chloroform on GO. For these tests the chloroform-GO system described as number II of Figure 4 is used. In this test all calculations use the same parameter values as the production runs (“Test setup 0”) except for one parameter, the parameter indicated in the key of the figure. Lines are for ease of identification.

energy E_b. For each of the systems I to XVI the term $-\Delta E_c^{\rm nl}$ contributes approximately double the binding energy. For example, in structure VIII the term $-\Delta E_c^{\rm nl}$ contributes 0.428 eV to the total 0.243 eV binding energy, the repulsion causing the offset. If E_b is affected by water, it must thus be affected through $-\Delta E_c^{\rm nl}$.

Water is not expected to affect $-\Delta E_c^{\rm nl}$. We argue that water can be described through the frequency-dependent relative dielectric constant of water, $\varepsilon(\omega)$. The term $E_c^{\rm nl}$ is calculated from the sum of poles in a contour integral in the space of complex frequencies. The sum starts at frequencies above the plasmon frequency,[41–43] i.e., at frequencies above ~ 10 eV. While the static value of the water dielectric constant $\varepsilon(\omega = 0)$ is around 80, it falls off to about 1.8 at optical frequencies (the visible-light index of refraction 1.333 squared), and at even larger frequencies $\varepsilon(\omega)$ asymptotically goes to the value 1, based on the f-sum rule.[44] The effect of water is thus small in adsorption systems where the nonlocal correlation $-\Delta E_c^{\rm nl}$ dominates the binding: the relevant frequencies are much too high for the water molecules to engage in the vibrations and they do not change the nonlocal interaction.

In line with the argument that the interaction between chloroform and GO is dominated by the (dynamic) nonlocal correlation interaction we find, below, that the (static) dipole of the full system is so small that it does not interact with similar dipoles of the periodically repeated images of the system (in the direction perpendicular to GO). Our main calculations are carried out without correction for such dipole-dipole interaction. The effect is tested by applying a dipole correction along the z-axis, for a couple of our systems, in a manner described in Refs.

AIP Publishing

This manuscript was accepted by J. Chem. Phys. Click here to see the version of record.

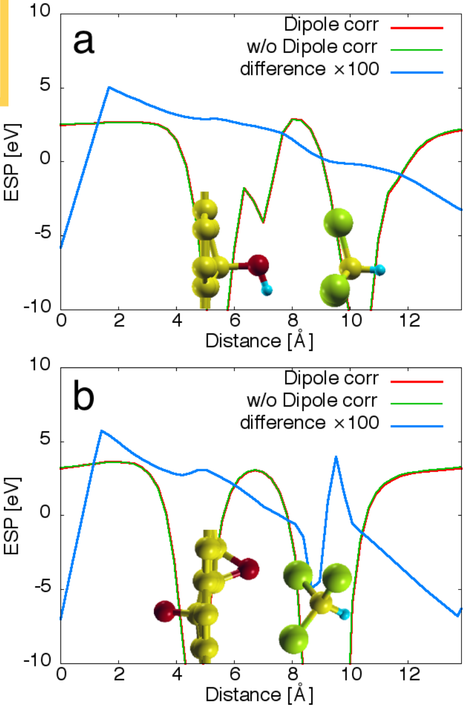

FIG. 6. Effect of the dipole correction on the electrostatic potential in GO-chloroform systems. The plot shows a potential line scan along the box z-axis through the chloroform C atom (perpendicular to graphene) for the systems (a) II and (b) IV shown in Figure 4. To illustrate the length scales and positions of the constituents a piece of the GO slab and the chloroform molecule are placed at their position along the z-axes. The unit cell lengths in these two calculations are 16 Å (top) and 14 Å (bottom). Atom colors as in Figure 4. The solid blue line shows 100× the difference in potentials with and without the dipole correction.

45 and 46. In Figure 6 we show the results of two such dipole correction tests, by plotting the electrostatic potential (ESP) curves with and without dipole correction. In each of the panels the two ESP curves (with and without dipole correction) are almost overlapping, and hence, for clarity we also plot 100× the difference. We see that the dipole correction only has minor effects on the ESP of the studied systems. In other words, the total system (GO and chloroform) does not carry a dipole. This is not a trivial result, because by themselves the GO slab and chloroform are both polar objects. However, calculating the difference in binding energies with and without an applied dipole correction we find a difference of only 0.5–1.0 meV in most of the studied systems, with one exception showing a less than 10 meV difference.

IV. CONCLUSIONS

We present a computational study of chloroform physisorption on GO, using DFT calculations with the vdW-DF-cx method. The binding energy values vary from approximately 0.20 to 0.40 eV, and depend both on the local environment on the GO, as well as the orientation of the chloroform molecule relative to GO. We find that these results are not influenced by the inclusion of water (as a continuum described by the dielectric constant $\varepsilon(\omega)$) in the system. Thus we find that chloroform physisorbs rather strongly on GO and that GO has potential as filtering material for chlorinated water.

We also document the ability of vdW-DF-cx of balancing the sp^2 and sp^3 bindings of the C atoms in GO. We do this by comparing the formation energy of the unsaturated GO structures, both in the semilocal PBE and the nonlocal vdW-DF-cx functionals: going from pure sp^2 binding in clean graphene to a mixture of sp^2 and sp^3, in the formation of unsaturated GO. The GO structures are structurally relaxed. Besides a small offset in the formation energies common to all the structures, we find the same formation energies of GO in both PBE and vdW-DF-cx calculations, underlining the ability of vdW-DF-cx of handling the change from sp^2 to sp^3 bindings just as well as PBE does.

The information that we obtain from studies of the physisorption of small molecules, like in this study the binding energies and the orientation of chloroform, may be useful both as direct results, but also as input for modeling of larger systems.[47] While our study is not exhaustive in searching for all possible physisorption geometries we have included a number of structures such that we have covered many of the relevant local environments of GO functional groups.

ACKNOWLEDGMENTS

We thank Per Hyldgaard and Kristian Berland for providing access to a pre-release version of the vdW-DF-cx code with Quantum Espresso. Support from the Swedish Research Council (VR) and from the Knut and Alice Wallenberg Foundation (KAW) is gratefully acknowledged. The computations were performed on resources at Chalmers Centre for Computational Science and Engineering (C3SE) provided by the Swedish National Infrastructure for Computing (SNIC).

[1] B. C. Brodie, Phil. Trans. R. Soc. Lond. **149**, 249 (1859).

[2] S. Stankovich, D. A. Dikin, G. H. B. Dommett, K. M. Kohlhaas, E. J. Zimney, E. A. Stach, R. D. Piner, S. Nguyen, and R. S. Ruoff, Nature **442**, 282 (2006).

[3] S. Stankovich, R. D. Piner, X. Q. Chen, N. Q. Wu, S. T. Nguyen, and R. S. Ruoff, J. Mater. Chem. **16**, 155 (2006).

[4] H. C. Schniepp, J. L. Li, M. J. McAllister, H. Sai, M. Herrera-Alonso, D. H. Adomson, R. K. Prud'homme, R. Car, D. A. Saville, and I. A. Aksay, J. Phys. Chem. B **110**, 8535 (2006).

[5] C. Gómez-Navarro, R. T. Weitz, A. M. Bittner, M. Scolari, A. Mews, M. Burghard, and K. Kern, Nano Lett. **7**, 3499 (2007).

[6] A. Lerf, H. He, M. Forster, and J. Klinowski, J. Phys. Chem. B **102**, 4477 (1998).

[7] T. Szabó, O. Berkesi, P. Forgo, K. Josepovits, Y. Sanakis, D. Petridis, and I. Dekany, Chem. Mater. **18**, 2740 (2006).

[8] J. T. Paci, T. Belytschko, and G. C. Schatz, J. Phys. Chem. C **111**, 18099 (2007).

[9] D. W. Boukhvalov and M. I. Katsnelson, JACS **130**, 10697 (2008).

[10] K. A. Mkhoyan, A. W. Contryman, J. Silcox, D. A. Stewart, G. Eda, C. Mattevi, S. Miller, and M. Chhowalla, Nano Lett. **9**, 1058 (2009).

[11] D. R. Dreyer, S. Park, C. Bielawski, and R. S. Ruoff, Chem. Soc. Rev. **39**, 228 (2009).

[12] L. Wang, Y. Y. Sun, K. Lee, D. West, Z. F. Chen, J. J. Zhao, and S. B. Zhang, Phys. Rev. B **82**, 161406 (2010).

[13] Y. Zhu, S. Murali, W. Cai, X. Li, J. W. Suk, J. R. Potts, and R. S. Ruoff, Adv. Mater. **22**, 3906 (2010).

[14] S. Basu and P. Bhattacharyya, Sensors Actuators B: Chemical **173**, 1 (2012).

[15] S. M. Maliyekkal, T. S. Sreeprasad, D. Krishnan, S. Kouser, A. K. Mishra, U. V. Waghmare, and T. Pradeep, Small **9**, 273 (2012).

[16] R. K. Joshi, P. Carbone, F. C. Wang, V. G. Kravets, Y. Su, I. V. Grigorieva, H. A. Wu, A. K. Geim, and R. R. Nair, Science **343**, 752 (2014).

[17] M. Rossberg, W. Lendle, G. Pfleiderer, A. Tögel, T. R. Torkelson, and K. K. Beutel, "Chloromethanes," (Wiley-VCH Verlag GmbH & Co. KGaA, Weinheim, 2012).

[18] M. Rossberg, W. Lendle, G. Pfleiderer, A. Tögel, E.-L. Dreher, E. Langer, H. Rassaerts, P. Kleinschmidt, H. Strack, R. Cook, U. Beck, K.-A. Lipper, T. R. Torkelson, E. Löser, and K. K. Beutel (Wiley-VCH Verlag GmbH & Co. KGaA, Weinheim, 2006) Chap. Chlorinated Hydrocarbons.

[19] J. P. Perdew, K. Burke, and M. Ernzerhof, Phys. Rev. Lett. **77**, 3865 (1996).

[20] M. Dion, H. Rydberg, E. Schröder, D. C. Langreth, and B. I. Lundqvist, Phys. Rev. Lett. **92**, 246401 (2004).

[21] M. Dion, H. Rydberg, E. Schröder, D. C. Langreth, and B. I. Lundqvist, Phys. Rev. Lett. **95**, 109902 (2005).

[22] T. Thonhauser, V. R. Cooper, S. Li, A. Puzder, P. Hyldgaard, and D. C. Langreth, Phys. Rev. B. **76**, 125112 (2007).

[23] K. Berland, C. A. Arter, V. R. Cooper, K. Lee, B. I. Lundqvist, E. Schröder, T. Thonhauser, and P. Hyldgaard, J. Chem. Phys. **140**, 18A539 (2014).

[24] K. Berland, V. R. Cooper, K. Lee, E. Schröder, T. Thonhauser, P. Hyldgaard, and B. I. Lundqvist, Rep. Prog. Phys. **78**, 066501 (2015).

[25] K. Berland and P. Hyldgaard, Phys. Rev. B **89**, 035412 (2014).

[26] H. Ulbricht, R. Zacharia, N. Cindir, and T. Hertel, Carbon **44**, 2931 (2006).

[27] A. Fujii, K. Shibasaki, T. Kazama, R. Itaya, N. Mikami, and S. Tsuzuki, Phys. Chem. Chem. Phys. **10**, 2836 (2008).

[28] T. R. Rybolt, D. L. Logan, M. W. Milburn, H. E. Thomas, and A. B. Waters, J. Colloid Interface Sci. **220**, 148 (1999).

[29] J. Åkesson, O. Sundborg, O. Wahlström, and E. Schröder, J. Chem. Phys. **137**, 174702 (2012).

[30] J. Hooper, V. R. Cooper, T. Thonhauser, N. A. Romero, F. Zerilli, and D. C. Langreth, ChemPhysChem **9**, 891 (2008).

[31] Y. Peng and J. Li, Front. Environ. Sci. Eng. **7**, 403 (2013).

[32] T. Nakajima and Y. Matsuo, Carbon **26**, 357 (1988).

[33] A. Kokalj, Comp. Mater. Sci. **28**, 155 (2003).

[34] W. Humphrey, A. Dalke, and K. Schulten, J. Molecular Graphics **14**, 33 (1996).

[35] P. Giannozzi, S. Baroni, N. Bonini, M. Calandra, R. Car, C. Cavazzoni, D. Ceresoli, G. L. Chiarotti, M. Cococcioni, I. Dabo, A. D. Corso, S. Fabris, G. Fratesi, S. de Gironcoli, R. Gebauer, U. Gerstmann, C. Gougoussis, A. Kokalj, M. Lazzeri, L. Martin-Samos, N. Marzari, F. Mauri, R. Mazzarello, S. Paolini, A. Pasquarello, L. Paulatto, C. Sbraccia, S. Scandolo, G. Sclauzero, A. P. Seitsonen, A. Smogunov, P. Umari, and R. M. Wentzcovitch, J. Phys.: Condens. Matter **21**, 395502 (2009).

[36] Open-source DFT code QE, `http://www.quantum-espresso.org/`, version 5.0.2, with a local addition for vdW-DF-cx calculations, and version 5.3.0 for calculating the effect of spin.

[37] D. Vanderbilt, Phys. Rev. B **41**, 7892 (1990).

[38] K. Garrity, J. Bennett, K. Rabe, and D. Vanderbilt, Comput. Mater. Sci. **81**, 446 (2014).

[39] Ž. Šljivančanin, A. S. Milošević, Z. S. Popović, and F. R. Vukajlović, Carbon **54**, 482 (2013).

[40] J. Rossmeisl, A. Logadottir, and J. Nørskov, Chem. Phys. **319**, 178 (2005).

[41] P. Hyldgaard, K. Berland, and E. Schröder, Phys. Rev. B (2014), in press.

[42] A. C. Maggs and N. W. Ashcroft, Phys. Rev. Lett. **59**, 113 (1987).

[43] K. Rapcewicz and N. W. Ashcroft, Phys. Rev. B **44**, 4032 (1991).

[44] D. Wagner, J. Phys. C Solid State **8**, 1829 (1975).

[45] L. Bengtsson, Phys. Rev. B **59**, 12301 (1999).

[46] B. Meyer and D. Vanderbilt, Phys. Rev. B **63**, 205426 (2001).

[47] V. R. Cooper, Y. Ihm, and J. R. Morris, Phys. Proc. **34**, 34 (2012).

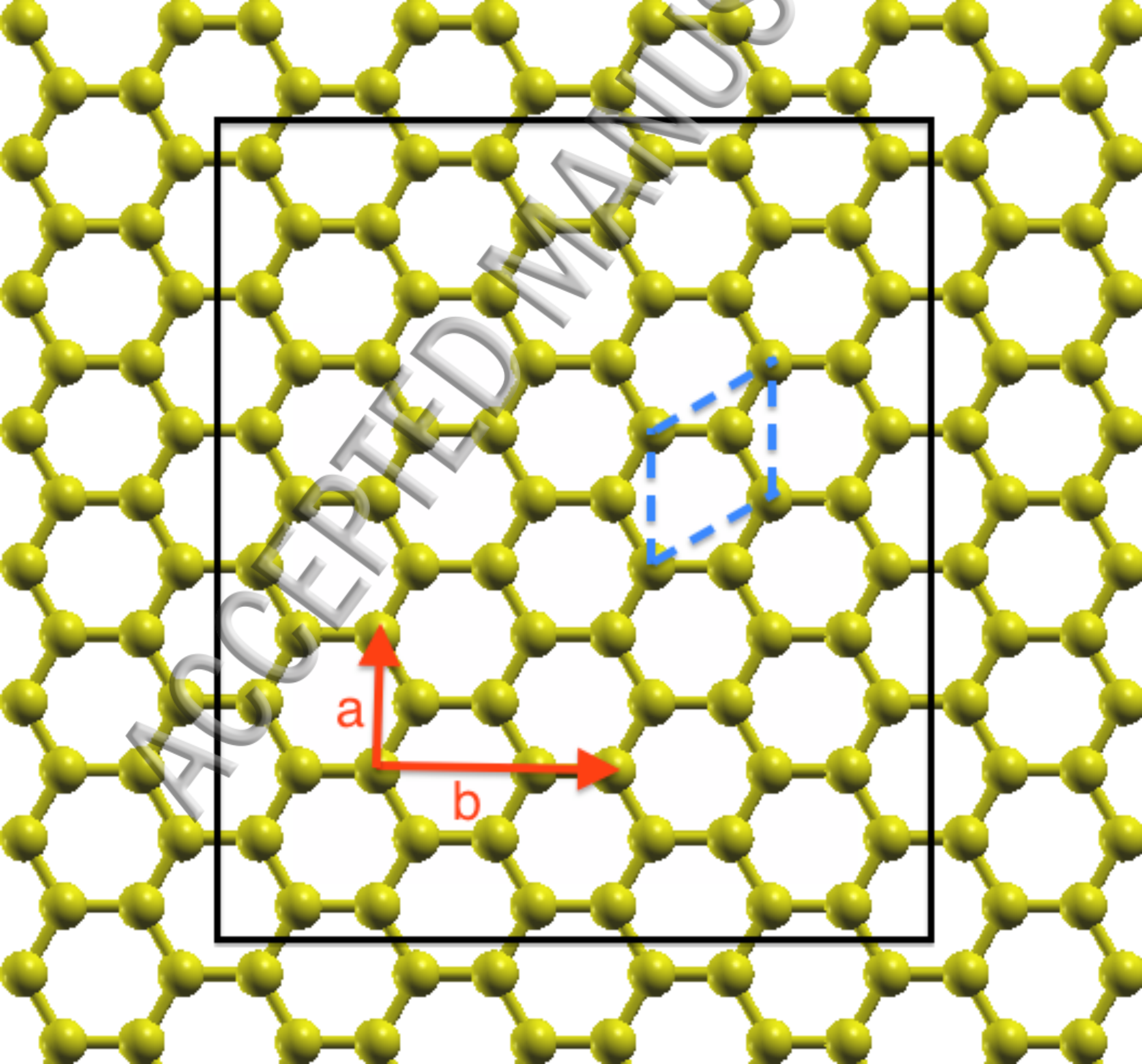
a
b

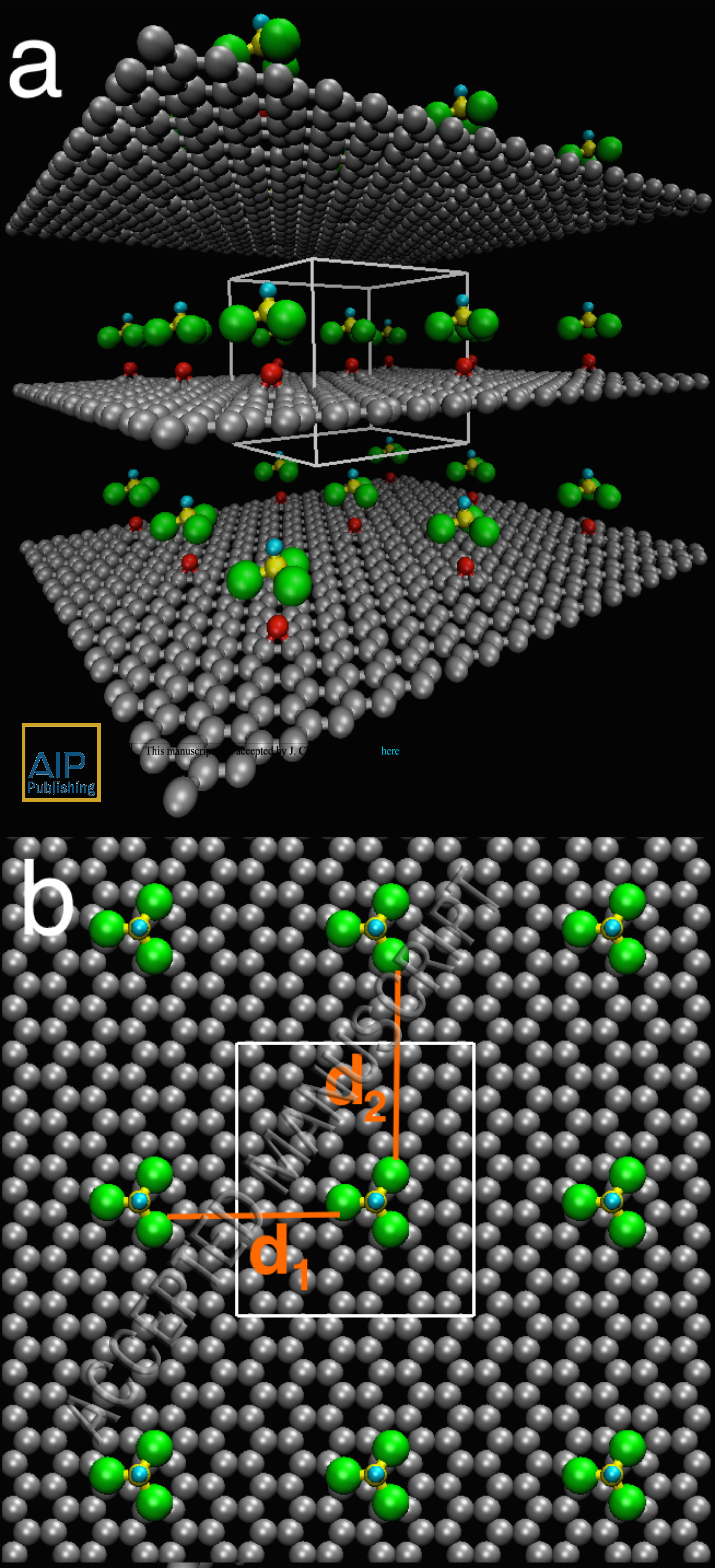

AIP Publishing
This manuscript was accepted by J. Chem. Phys. Click here
ACCEPTED MANUSCRIPT

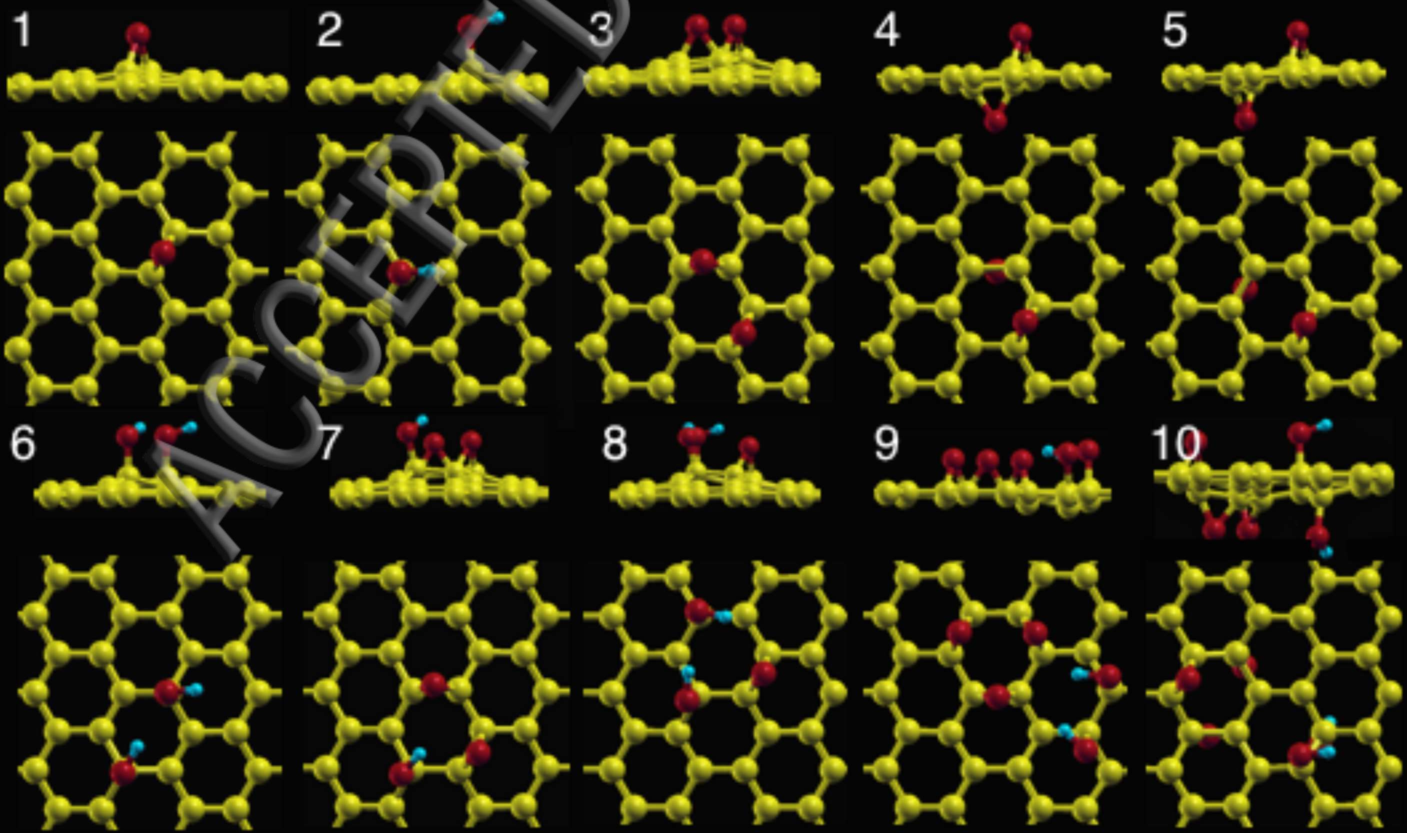
1
2
3
4
5
6
7
8
9
10

ACCEPTED

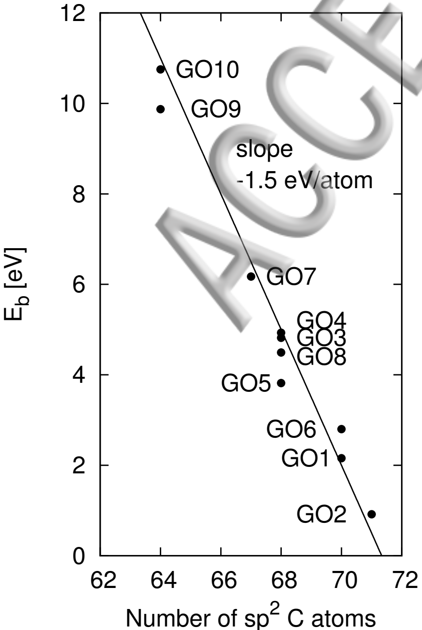
GO10
GO9
slope
-1.5 eV/atom
GO7
GO4
GO3
GO8
GO5
GO6
GO1
GO2
E_b [eV]
0
2
4
6
8
10
12
62
64
66
68
70
72
Number of sp^2 C atoms

ACCE

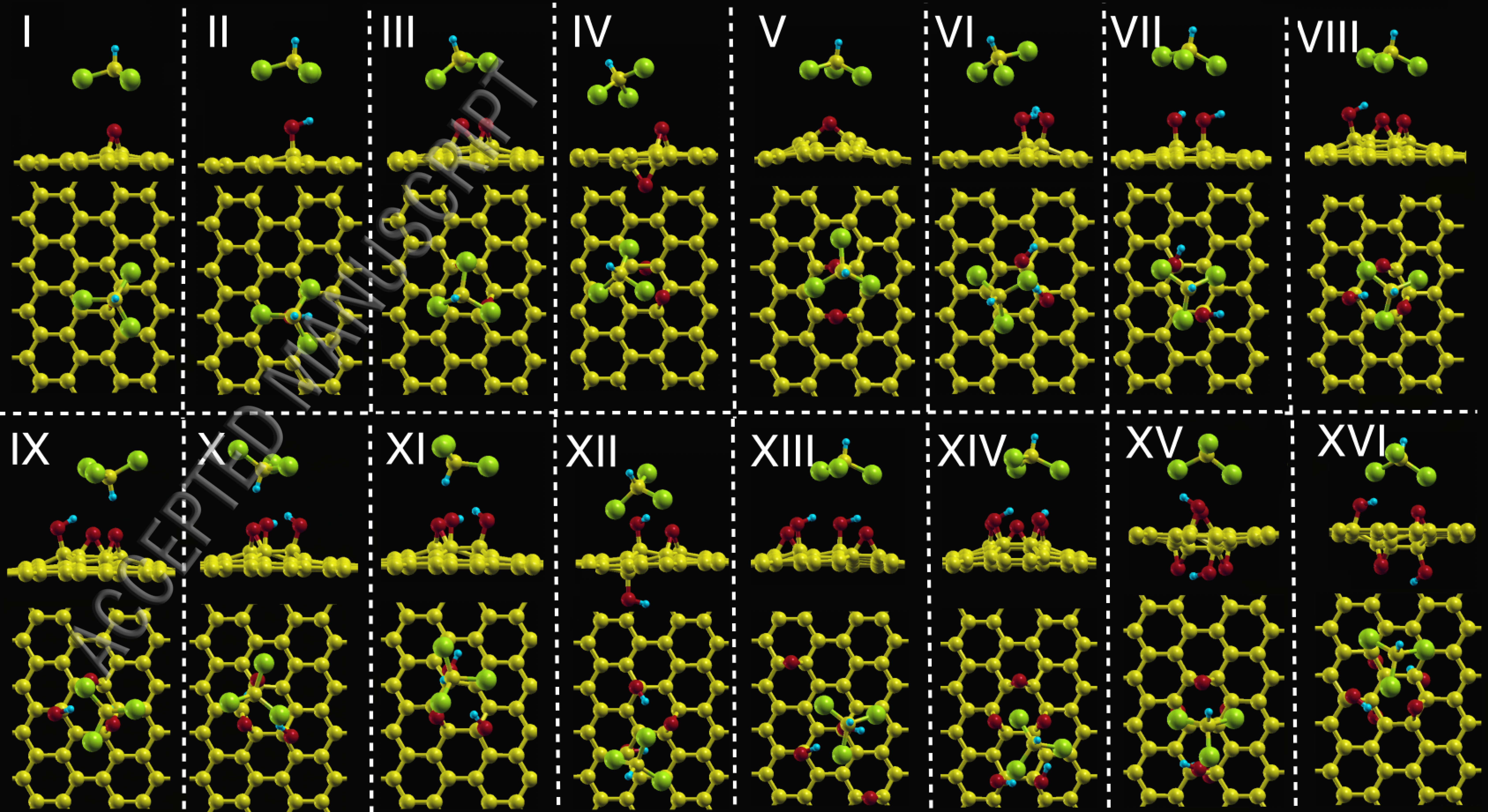
I
II
III
IV
V
VI
VII
VIII
IX
X
XI
XII
XIII
XIV
XV
XVI

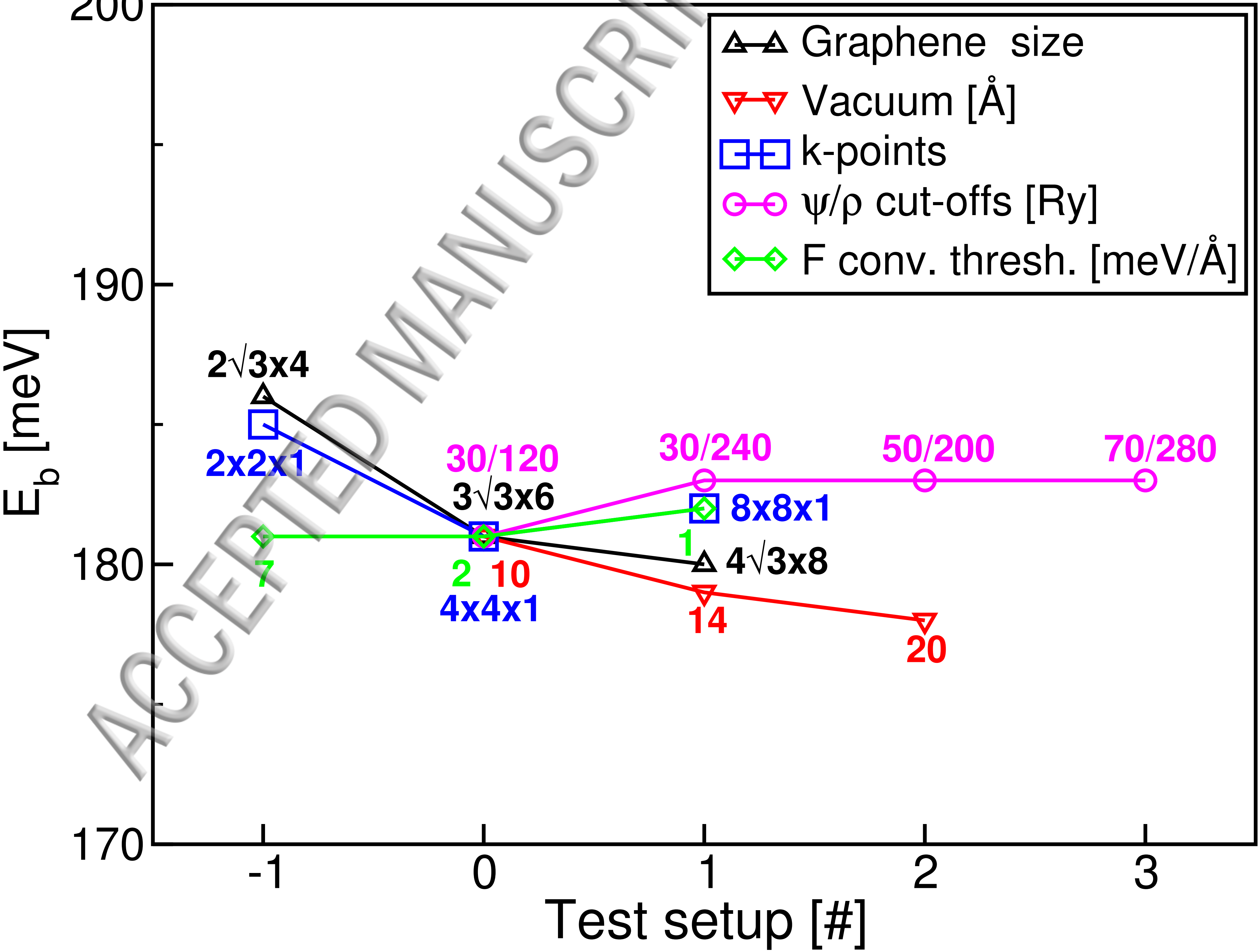

200
190
180
170
E_b [meV]
-1
0
1
2
3
Test setup [#]
Graphene size
Vacuum [Å]
k-points
ψ/ρ cut-offs [Ry]
F conv. thresh. [meV/Å]
2√3x4
2x2x1
7
30/120
3√3x6
2
10
4x4x1
30/240
8x8x1
1
4√3x8
14
50/200
20
70/280

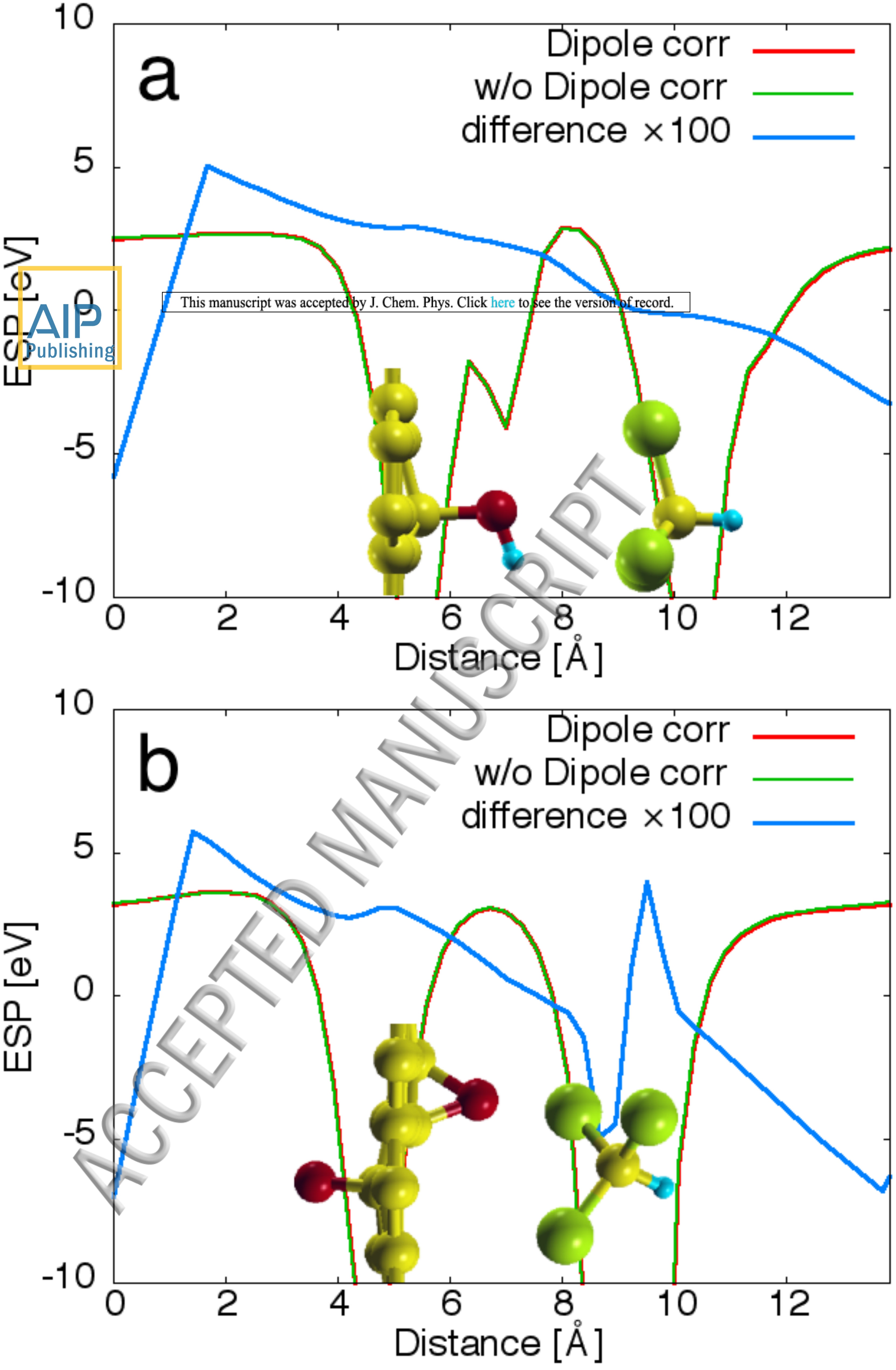AIP Publishing